

# Inherent Enhancement of Electronic Emission from Hexaboride Heterostructure

Johannes Voss,<sup>1,2,\*</sup> Aleksandra Vojvodic,<sup>1,2</sup> Sharon H. Chou,<sup>3</sup> Roger T. Howe,<sup>3</sup> and Frank Abild-Pedersen<sup>2,†</sup>

<sup>1</sup>*Department of Chemical Engineering, Stanford University, Stanford, California 94305, USA*

<sup>2</sup>*SUNCAT Center for Interface Science and Catalysis, SLAC National Accelerator Laboratory, Menlo Park, California 94025, USA*

<sup>3</sup>*Department of Electrical Engineering, Stanford University, Stanford, California 94305, USA*

(Received 1 May 2014; published 6 August 2014)

Based on a nonequilibrium Green's-function approach to the calculation of emission currents from first principles, we show that cathodes consisting of  $\text{LaB}_6/\text{BaB}_6$  superlattices can yield an order-of-magnitude higher thermionic current densities than pure  $\text{LaB}_6$  cathodes. Because of a 0.46-eV lowering of the work function, such a heterostructure cathode could thus be operated at significantly lower temperatures. Neither the stability nor the magnitude of electronic tunneling coefficients is compromised in the superlattice system as compared to pure  $\text{LaB}_6$ , which is in contrast to the generally reduced stability and large dipole barriers in the case of adsorbate-induced lowering of the work function. The heterostructure could thus be used as a cathode material that at the same time is stable and has emission properties superior to those of pure  $\text{LaB}_6$ .

DOI: 10.1103/PhysRevApplied.2.024004

## I. INTRODUCTION

Lanthanum hexaboride  $\text{LaB}_6$  is one of the most-often-used cathode materials in thermionic emitters [1,2], and it has also been demonstrated to provide a bright source for field emission in the form of emitter arrays [3] and nanowires [4–7]. The advantages of  $\text{LaB}_6$  as a cathode material lie in the fact that it exhibits both thermal stability and a low work function of its most stable surface orientation [100] [8,9]. This behavior is in contrast to, e.g., the trends in the periodic table, where low work function always means a relatively low melting point. In addition, the evaporation rate of surface atoms is low even at elevated temperatures and similar for La and B atoms [10–12], such that the [100] surface remains terminated with La atoms over time [13].

The emission properties of  $\text{LaB}_6$  could be improved by lowering its work function, either through adsorbates or through modification of the bulk structure. Adsorption of alkali or alkali-earth atoms can reduce the work function of metal surfaces significantly through the formation of strong surface dipoles. This mechanism is particularly effective if the bare-metal surface has a high work function, leading to a large dipole due to transfer of the loosely bound outer  $s$  electrons of the adsorbates. If the work function of the bare metal is low—which is the case for  $\text{LaB}_6(100)$ —the binding of the adsorbates will be relatively weak and the induced surface dipoles will be small. Adsorbing, e.g., a monolayer of O on  $\text{LaB}_6(100)$  first and then adsorbing Cs increases the desorption temperature of Cs to about 1000 K,

but the observed work function is more than 1 eV higher than that of bare  $\text{LaB}_6(100)$ , since the O layer causes an increase in the work function [14].

Alloying of  $\text{LaB}_6$  with other hexaborides has also been considered to improve emission [15–22]. First studies of such mixed hexaborides, where the crystals were grown from aluminum flux [16,23], did not yield an increase in thermionic current densities [15]. According to density-functional-theory (DFT) calculations, replacing La with Ba in the surface layer should decrease the work function [24], however, such a surface layer would evaporate within seconds at elevated temperatures [12]. Later experiments demonstrated bulk substitution of Ba for La in  $\text{LaB}_6$  using a spark-plasma sintering process with an increase of the lattice constants of the hexaboride [25], and Liu *et al.* [18] showed enhanced thermionic emission of  $\text{LaB}_6$  and  $\text{BaB}_6$  mixtures (for the latter experiments, no crystal structure analysis was provided).

Here, we show based on DFT calculations that epitaxial  $\text{LaB}_6/\text{BaB}_6$  superstructures are more stable than their phase-separated constituents and that the work function of such a structure is 0.46 eV lower than that of pure  $\text{LaB}_6$ . Using first-principles transport calculations, we find that the tunneling probabilities are of the same magnitude as those for pure  $\text{LaB}_6$  despite the lowered work function. This  $\text{LaB}_6/\text{BaB}_6$  heterostructure would thus provide a cathode material combining good stability with emission properties superior to those of pure  $\text{LaB}_6$ .

## II. DETAILS OF CALCULATION

DFT calculations are performed with the DACAPO [26] ultrasoft pseudopotential [27] code, using the Perdew-Burke-Ernzerhof [28] exchange-correlation functional.

\*vossj@slac.stanford.edu

†abild@slac.stanford.edu

Kohn-Sham states are expanded in plane-wave basis sets with a cutoff of 400 eV (benchmark calculations using hard projector-augmented wave potentials [29] as implemented in the QUANTUM ESPRESSO [30] code at a plane-wave cutoff of 2000 eV differ by less than 50 meV from the work functions obtained with the softer ultrasoft pseudopotentials used here). For the optimization of lattice constants, an increased cutoff of 800 eV is used to reduce spurious Pulay stress [31]. Brillouin zones are sampled with  $k$ -point spacings of at most  $\sim 0.1 \text{ \AA}^{-1}$ . Fermi surface smearing is performed using Fermi-Dirac statistics with temperatures  $k_B T \geq 0.1 \text{ eV}$  ( $k_B$  denotes Boltzmann's constant) to determine the temperature dependence of the Fermi level. Transformation of Bloch states to Wannier functions used in the transport calculations is performed with the ASE software package [32,33].

The transport calculations are based on a recently developed [34] nonequilibrium Green's-function approach [35,36], where bulk metallic lead and vacuum are treated as semi-infinite systems. Bulk metal and vacuum are the source and drain for electrons, respectively. Using the Landauer-Büttiker formalism [37,38], we calculate the thermionic current density as

$$J(T) = \frac{1}{\pi S} \int dE f[E - \mu(T), T] \mathcal{T}(E), \quad (1)$$

where the metallic lead and vacuum are held at temperatures  $T$  and 0 K, respectively. The temperature dependence of the work function of the slab is taken into account here only through the temperature dependence of the Fermi level  $\mu(T)$ .  $f[E - \mu(T), T]$  is the Fermi-Dirac distribution.  $\mathcal{T}(E)$  is the transmission function of the considered surface with surface area  $S$ . The calculation of  $\mathcal{T}(E)$  is based on DFT Hamiltonians in Wannier-function basis sets for metallic lead and slab, while the vacuum states are represented as plane waves (see Ref. [34] for details). We neglect thermal expansion of the lattice, which is a good approximation due to a low expansion coefficient of  $\text{LaB}_6$  of  $6 \times 10^{-6} \text{ K}^{-1}$  [39].

For  $\text{LaB}_6$  and  $\text{LaB}_6/\text{BaB}_6$ , the considered slabs consist of four and five layers of hexaboride with an additional terminating layer of La and Ba, respectively. The two topmost hexaboride layers are allowed to relax, and a dipole correction [40] is applied.

### III. RESULTS

#### A. Thermodynamic properties

We consider heterostructures with alternating single layers of  $\text{LaB}_6$  and  $\text{BaB}_6$ , i.e., with chemical formula  $\text{LaBaB}_{12}$ . Based on DFT total-energy calculations of bulk structures with alternating layers, we find that the [100] growth direction would be energetically preferred over the [110] and [111] directions by 65 and 24 meV per formula unit  $\text{LaBaB}_{12}$ , respectively. We will thus focus on the

heterostructure with [100] as layer normal, and it will hence be straightforward to directly compare structural properties such as relaxation of the (100) surfaces of  $\text{LaB}_6$  and  $\text{LaB}_6/\text{BaB}_6$ .

The bulk structure of  $\text{LaB}_6/\text{BaB}_6$  with growth direction [100] is 0.18 eV more stable per formula unit  $\text{LaBaB}_{12}$  than phase-separated  $\text{LaB}_6$  and  $\text{BaB}_6$ . The DFT-optimized lattice constants are 8.39 Å for the [100] and 4.19 Å for the perpendicular directions. The optimized lattice constants of  $\text{LaB}_6$  and  $\text{BaB}_6$  are 4.15 and 4.24 Å, respectively. The lattice spacing in the heterostructure is approximately the arithmetic mean of the spacing in the constituent hexaboride phases.

To calculate the preferred termination of the  $\text{LaB}_6/\text{BaB}_6(100)$  surface, we consider a slab terminated by Ba atoms on one face and by La atoms on the other. Referencing to the cohesive energies of bulk Ba and La, removal of the  $\text{BaB}_6$  surface layer is 0.4 eV more expensive per hexaboride unit than removing the  $\text{LaB}_6$  surface layer on the other face. Termination of the heterostructure with Ba atoms is thus thermodynamically preferred (termination with B atoms is several eV more expensive per removed Ba atom). The corresponding Ba-terminated surface is depicted in Fig. 1. When surface layers begin to evaporate at elevated temperatures, there will be a strong thermodynamic driving force for diffusion of Ba atoms to the surface: the energy of the La-terminated system is lowered by 0.28 eV for exchange of a surface La atom with a subsurface Ba atom. Therefore, the  $\text{LaB}_6/\text{BaB}_6(100)$  surface should be replenished with terminating Ba atoms during thermionic operation.

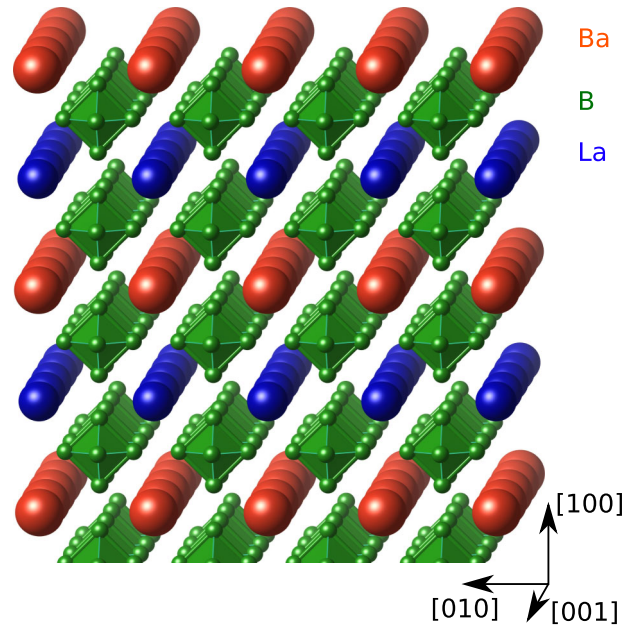


FIG. 1. Scheme [41] of the Ba-terminated  $\text{LaB}_6/\text{BaB}_6$  surface with growth direction [100]. La is depicted by blue spheres, Ba by orange spheres, and  $\text{B}_6$  octahedra are represented in green color.

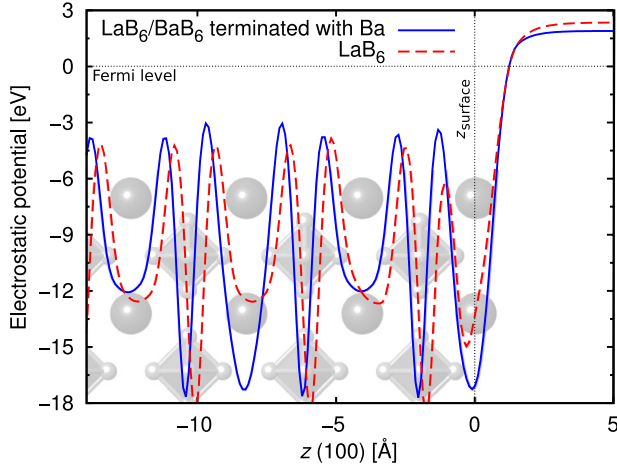


FIG. 2. Average electrostatic potential along the [100] direction of Ba-terminated  $\text{LaB}_6/\text{BaB}_6(100)$  and  $\text{LaB}_6(100)$ . The horizontal and vertical dotted lines represent the Fermi level and the position of the surface atoms, respectively. The gray spheres and octahedra in the background depict the atomic positions of La/Ba and B in  $\text{LaB}_6/\text{BaB}_6$ , respectively (the lattice spacing in  $\text{LaB}_6$  is smaller).

### B. Electronic properties

Not only is the termination of the  $\text{LaB}_6/\text{BaB}_6$  heterostructure with Ba atoms thermodynamically preferred, but it also leads to a lower work function of 1.89 eV as compared to termination with La atoms, which has a work function of 2.30 eV (Table I). The strong driving force for diffusion of Ba to the surface is thus important for maintaining the lowest-possible work function of this material under thermionic emission operation conditions. The Ba-terminated, stable  $\text{LaB}_6/\text{BaB}_6(100)$  surface has a 0.46-eV-lower work function than pure  $\text{LaB}_6$  (Fig. 2; the La-terminated heterostructure only has a 0.05-eV-lower work function than pure  $\text{LaB}_6$ ). The work function of the heterostructure is 0.34 eV lower than the work function of  $\text{BaB}_6(100)$ . The Ba-terminated  $\text{LaB}_6/\text{BaB}_6$  heterostructure

TABLE I. Work functions of  $\text{LaB}_6(100)$  and Ba- and La-terminated  $\text{LaB}_6/\text{BaB}_6(100)$ . Both the values for slabs with atoms at bulk positions and relaxed slabs are shown. The Ba-terminated heterostructure has the lowest work function. There is a strong thermodynamic driving force for diffusion of Ba atoms to the surface as described in the text, such that the surface of the heterostructure will be replenished with Ba atoms during thermionic operation.

Structure	Termination	Work function (eV, relaxed)	Work function (eV, unrelaxed)
$\text{LaB}_6$	La	2.35	2.73
$\text{BaB}_6$	Ba	2.23	2.05
$\text{LaB}_6/\text{BaB}_6$	La	2.30	2.58
$\text{LaB}_6/\text{BaB}_6$	Ba	1.89	1.75

thus has a lower work function than both the constituent phases.

For pure  $\text{LaB}_6$ , relaxation at the  $\text{LaB}_6(100)$  surface leads to an inward movement of the terminating La atoms by about 0.3 Å. This relaxation leads to an increase in hybridization between the surface La  $6s, 5d$  and subsurface B  $2s, 2p$  states, which form a surface band common to hexaborides due to dangling B bonds [9,12,42,43]. This increase in hybridization due to relaxation can be seen in the increase in DOS at about 2 eV below the Fermi level shown in the top panel of Fig. 3. Despite the inward movement of the surface La atoms, surface relaxation reduces the work function due to redistribution of charge from the surface La atoms to this surface band [9,12,42]. The work function of  $\text{LaB}_6(100)$  without surface relaxation would be 2.73 eV, the charge redistribution induced by surface relaxation reduces the work function by 0.38 eV.

In the case of Ba-terminated  $\text{LaB}_6/\text{BaB}_6(100)$ , the inward movement of the terminating Ba atoms is less than 0.1 Å, and there is little change due to relaxation in the before-mentioned surface band (bottom panel of Fig. 3). In contrast to pure  $\text{LaB}_6(100)$ , the work function increases due to surface relaxation from 1.75 to 1.89 eV, since there is no charge redistribution to compensate the dipole reduction

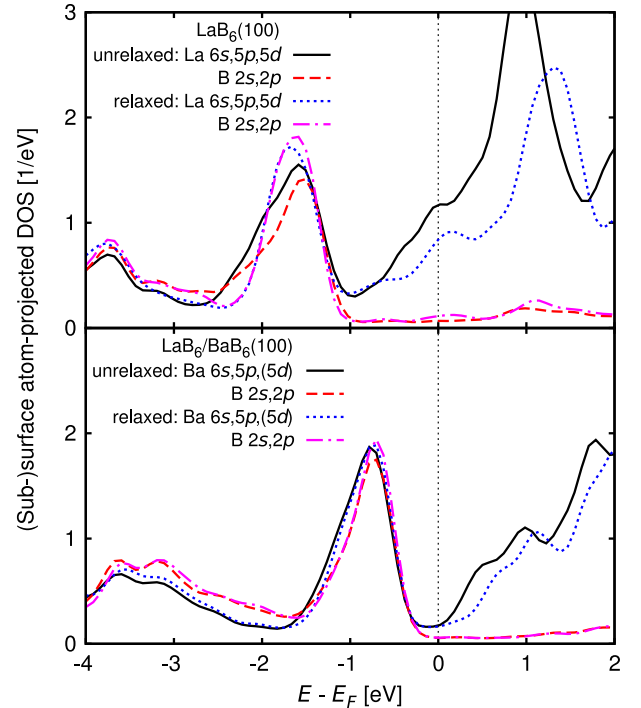


FIG. 3. Surface and subsurface atom-projected DOS for  $\text{LaB}_6(100)$  (top panel) and  $\text{LaB}_6/\text{BaB}_6(100)$  terminated with Ba (bottom panel). The DOS for both the unrelaxed (atoms at bulk coordinates) and the relaxed structures is shown. At approximately  $-2$  and  $-1$  eV, the DOS shows the surface bands due to dangling B bonds for  $\text{LaB}_6(100)$  and Ba-terminated  $\text{LaB}_6/\text{BaB}_6(100)$ , respectively.

due to the inward movement of the surface atoms. Hence, the electronic mechanism responsible for the work function lowering with surface relaxation in  $\text{LaB}_6$  is not active in the Ba-terminated heterostructure. Nevertheless, due to the large ionic radius of Ba, the surface dipole is larger for the Ba-terminated heterostructure to begin with, leading to the 0.46-eV-lower work function compared to  $\text{LaB}_6(100)$ . Generally, as summarized in Table I, both for the heterostructure and the pure hexaborides, La-terminated surfaces experience a work-function lowering due to surface relaxation, and Ba-terminated surfaces experience an increase in work function.

### C. Thermionic emission

We calculate thermionic current densities using Eq. (1), considering bulk  $\text{LaB}_6/\text{BaB}_6$  and  $\text{LaB}_6$  as metallic leads and surface slabs of the two materials as scattering regions, respectively.

The thermionic current densities are predicted to be an order of magnitude higher for  $\text{LaB}_6/\text{BaB}_6(100)$  than for  $\text{LaB}_6(100)$  (Fig. 4). A fit of the current densities to the Richardson-Dushman equation ( $\Phi$ : work function) [44]

$$J(T) = AT^2 \exp(-\Phi/k_B T), \quad (2)$$

yields a preexponential factor  $A$  of  $\sim 10 \text{ A/cm}^2/\text{K}^2$  both for  $\text{LaB}_6/\text{BaB}_6(100)$  and  $\text{LaB}_6(100)$ . Note that, in the definition of Eq. (2),  $A$  includes electronic reflection coefficients and to lowest order temperature dependence of the work function [44,45], which itself is considered temperature independent in Eq. (2) and also includes temperature dependence to lowest order. The lowering of the work function in the heterostructure thus does not lower the tunneling amplitudes, in contrast to the effect of dipole

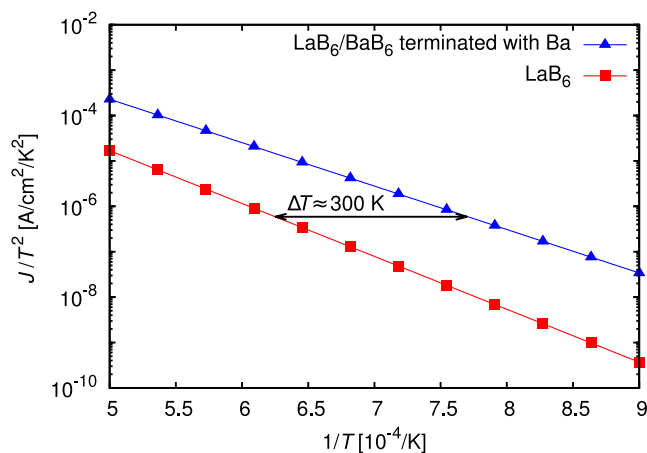


FIG. 4. Richardson-Dushman plot of thermionic emission from  $\text{LaB}_6/\text{BaB}_6(100)$  and  $\text{LaB}_6(100)$ . The arrow indicates by how much the working temperature of a  $\text{LaB}_6/\text{BaB}_6$  cathode could be lowered, yielding the same current densities as a  $\text{LaB}_6$  cathode at higher temperatures.

barriers in the case of work-function lowering through alkali-metal or alkali-earth-metal adsorption on, e.g., transition-metal surfaces [34].

Hence, the working temperatures for thermionic emission could be lowered significantly with  $\text{LaB}_6/\text{BaB}_6$  cathodes. To obtain, e.g., the same current density a pure  $\text{LaB}_6$  cathode would yield for  $T = 1600 \text{ K}$ , the working temperature could be lowered by 300 K with a  $\text{LaB}_6/\text{BaB}_6$  heterostructure cathode.

## IV. CONCLUSION

Based on first-principles calculations, we have shown that cathodes composed of  $\text{LaB}_6/\text{BaB}_6$  heterostructures have a significantly lower work function than pure  $\text{LaB}_6$  cathodes without sacrificing either thermodynamic stability or tunneling amplitudes. The low work function of  $\text{LaB}_6/\text{BaB}_6$  is an intrinsic property of the structure that does not depend on a work function lowering coating and will be maintained under thermionic emission conditions. The heterostructure cathodes could be operated at much lower temperatures than  $\text{LaB}_6$  cathodes, leading to a more efficient cathode with a potentially increased lifetime. The lower work function would also render  $\text{LaB}_6/\text{BaB}_6$  a more efficient field-emission cathode material than pure  $\text{LaB}_6$ .

## ACKNOWLEDGMENTS

This work is supported by grants from the Global Climate and Energy Project (GCEP) at Stanford University and the National Science Foundation Graduate Research Fellowship Program. J. V., A. V., and F. A. P. acknowledge financial support from the U.S. Department of Energy (DOE), Office of Basic Energy Sciences to the SUNCAT Center for Interface Science and Catalysis.

- [1] M. Trenary, "Surface science studies of metal hexaborides," *Sci. Tech. Adv. Mater.* **13**, 023002 (2012).
- [2] S. Yamamoto, "Fundamental physics of vacuum electron sources," *Rep. Prog. Phys.* **69**, 181 (2006).
- [3] M. Nakamoto and K. Fukuda, "Field electron emission from  $\text{LaB}_6$  and TiN emitter arrays fabricated by transfer mold technique," *Appl. Surf. Sci.* **202**, 289 (2002).
- [4] H. Zhang, J. Tang, Q. Zhang, G. Zhao, G. Yang, J. Zhang, O. Zhou, and L.-C. Qin, "Field emission of electrons from single  $\text{LaB}_6$  nanowires," *Adv. Mater.* **18**, 87 (2006).
- [5] H. Zhang, J. Tang, J. Yuan, J. Ma, N. Shinya, K. Nakajima, H. Murakami, T. Ohkubo, and L.-C. Qin, "Nanostructured  $\text{LaB}_6$  field emitter with lowest apical work function," *Nano Lett.* **10**, 3539 (2010).
- [6] X. H. Ji, Q. Y. Zhang, J. Q. Xu, and Y. M. Zhao, "Rare-earth hexaborides nanostructures: Recent advances in materials, characterization and investigations of physical properties," *Prog. Solid State Chem.* **39**, 51 (2011).

- [7] J. R. Brewer, R. M. Jacobberger, D. R. Diercks, and C. L. Cheung, "Rare earth hexaboride nanowires: General synthetic design and analysis using atom probe tomography," *Chem. Mater.* **23**, 2606 (2011).
- [8] H. Ahmed and A. N. Broers, "Lanthanum hexaboride electron emitter," *J. Appl. Phys.* **43**, 2185 (1972).
- [9] R. Nishitani, M. Aono, T. Tanaka, C. Oshima, S. Kawai, H. Iwasaki, and S. Nakamura, "Surface structures and work functions of the  $\text{LaB}_6$ (100), (110) and (111) clean surfaces," *Surf. Sci.* **93**, 535 (1980).
- [10] J. M. Lafferty, "Boride cathodes," *J. Appl. Phys.* **22**, 299 (1951).
- [11] E. Storms and B. Mueller, "Phase relationship, vaporization, and thermodynamic properties of the lanthanum-boron system," *J. Phys. Chem.* **82**, 51 (1978).
- [12] R. Monnier and B. Delley, "Properties of  $\text{LaB}_6$  elucidated by density functional theory," *Phys. Rev. B* **70**, 193403 (2004).
- [13] L. W. Swanson and D. R. McNeely, "Work functions of the (001) face of the hexaborides of Ba, La, Ce and Sm," *Surf. Sci.* **83**, 11 (1979).
- [14] S. A. Chambers, P. R. Davis, and L. W. Swanson, "Cesium and oxygen coadsorption on  $\text{LaB}_6$  single crystal surfaces: II. Thermal desorption of cesium from  $\text{LaB}_6$ (100)," *Surf. Sci.* **118**, 93 (1982).
- [15] M. Futamoto, M. Nakazawa, and U. Kawabe, "Thermionic emission properties of hexaborides," *Surf. Sci.* **100**, 470 (1980).
- [16] G. H. Olsen and A. V. Cafiero, "Single-crystal growth of mixed (La, Eu, Y, Ce, Ba, Cs) hexaborides for thermionic emission," *J. Cryst. Growth* **44**, 287 (1978).
- [17] P. H. Schmidt and D. C. Joy, "Low work function electron emitter hexaborides," *J. Vac. Sci. Technol.* **15**, 1809 (1978).
- [18] S. Liu, Q. Yang, W. Chen, J. Liu, and Z. Li, "Development of RE multiple boride  $(\text{La}_{0.55}\text{Ba}_{0.45})\text{B}_6$  and  $(\text{La}_{0.4}\text{Eu}_{0.6})\text{B}_6$  cathode materials," *Rare Met. Cement. Carbides* **34**, 8 (2006) [[http://en.cnki.com.cn/Article\\_en/CJFDTOTAL-XYJY200603003.htm](http://en.cnki.com.cn/Article_en/CJFDTOTAL-XYJY200603003.htm)].
- [19] S. Otani, H. Hiraoka, M. Ide, and Y. Ishizawa, "Thermionic emission properties of rare-earth-added  $\text{LaB}_6$  crystal cathodes," *J. Alloys Compd.* **189**, L1 (1992).
- [20] E. K. Storms, "Thermionic emission and vaporization behavior of the ternary systems of lanthanum hexaboride containing molybdenum boride, molybdenum diboride, zirconium diboride, gadolinium hexaboride, and neodymium hexaboride," *J. Appl. Phys.* **54**, 1076 (1983).
- [21] S. Zhou, J. Zhang, D. Liu, Q. Hu, and Q. Huang, "The effect of samarium doping on structure and enhanced thermionic emission properties of lanthanum hexaboride fabricated by spark plasma sintering," *Phys. Status Solidi A* **211**, 555 (2014).
- [22] G. V. Samsonov, A. I. Kondrashov, L. N. Okhremchuk, I. A. Podchernyaeva, N. I. Siman, and V. S. Fomenko, "Work function of  $\text{LaB}_6$ -based alloys," *J. Less-Common Met.* **67**, 415 (1979).
- [23] T. Aita, U. Kawabe, and Y. Honda, "Single crystal growth of lanthanum hexaboride in molten aluminium," *Jpn. J. Appl. Phys.* **13**, 391 (1974); M. Futamoto, T. Aita, and U. Kawabe, "Crystallographic properties of  $\text{LaB}_6$  formed in molten aluminium," *Jpn. J. Appl. Phys.* **14**, 1263 (1975).
- [24] M. A. Uijtewaal, G. A. de Wijs, and R. A. de Groot, "*Ab initio* and work function and surface energy anisotropy of  $\text{LaB}_6$ ," *J. Phys. Chem. B* **110**, 18459 (2006).
- [25] J. X. Zhang, S. L. Zhou, D. M. Liu, L. H. Bao, Y. F. Wei, R. G. Ma, and Q. Z. Huang, "Synthesis, characterization and properties of nanostructured  $(\text{La}_x\text{Ba}_{1-x})\text{B}_6$  cathode materials by liquid phase reactive spark plasma sintering," in *Proceedings of the 8th International Vacuum Electron Sources Conference and Nanocarbon (IVESC), 2010* (IEEE Press, Piscataway, NJ, 2010), pp. 175–177.
- [26] B. Hammer, L. B. Hansen, and J. K. Nørskov, "Improved adsorption energetics within density-functional theory using revised Perdew-Burke-Ernzerhof functionals," *Phys. Rev. B* **59**, 7413 (1999).
- [27] D. Vanderbilt, "Soft self-consistent pseudopotentials in a generalized eigenvalue formalism," *Phys. Rev. B* **41**, 7892 (1990).
- [28] J. P. Perdew, K. Burke, and M. Ernzerhof, "Generalized gradient approximation made simple," *Phys. Rev. Lett.* **77**, 3865 (1996).
- [29] P. E. Blöchl, "Projector augmented-wave method," *Phys. Rev. B* **50**, 17953 (1994).
- [30] P. Giannozzi, S. Baroni, N. Bonini, M. Calandra, R. Car, C. Cavazzoni, D. Ceresoli, G. L. Chiarotti, M. Cococcioni, I. Dabo, A. Dal Corso, S. de Gironcoli, S. Fabris, G. Fratesi, R. Gebauer, U. Gerstmann, C. Gougoussis, A. Kokalj, M. Lazzeri, and L. Martin-Samos *et al.*, "QUANTUM ESPRESSO: A modular and open-source software project for quantum simulations of materials," *J. Phys. Condens. Matter* **21**, 395502 (2009).
- [31] P. Pulay, "*Ab initio* calculation of force constants and equilibrium geometries in polyatomic molecules," *Mol. Phys.* **17**, 197 (1969).
- [32] K. S. Thygesen, L. B. Hansen, and K. W. Jacobsen, "Partly occupied Wannier functions," *Phys. Rev. Lett.* **94**, 026405 (2005).
- [33] S. R. Bahn and K. W. Jacobsen, "An object-oriented scripting interface to a legacy electronic structure code," *Comput. Sci. Eng.* **4**, 56 (2002); <https://wiki.fysik.dtu.dk>.
- [34] J. Voss, A. Vojvodic, S. H. Chou, R. T. Howe, I. Bargatin, and F. Abild-Pedersen, "Thermionic current densities from first principles," *J. Chem. Phys.* **138**, 204701 (2013).
- [35] H. Haug and A.-P. Jauho, *Quantum Kinetics in Transport and Optics of Semiconductors*, 2nd ed. (Springer, Berlin, 2008).
- [36] S. Datta, *Electronic Transport in Mesoscopic Systems* (Cambridge University Press, Cambridge, 1995).
- [37] R. Landauer, "Spatial variation of currents and fields due to localized scatterers in metallic conduction," *IBM J. Res. Dev.* **1**, 223 (1957); "Electrical resistance of disordered one-dimensional lattices," *Philos. Mag.* **21**, 863 (1970).
- [38] M. Büttiker, "Role of quantum coherence in series resistors," *Phys. Rev. B* **33**, 3020 (1986).
- [39] V. Craciun and D. Craciun, "Pulsed laser deposition of crystalline  $\text{LaB}_6$  thin films," *Appl. Surf. Sci.* **247**, 384 (2005).
- [40] J. Neugebauer and M. Scheffler, "Adsorbate-substrate and adsorbate-adsorbate interactions of Na and K adlayers on Al(111)," *Phys. Rev. B* **46**, 16067 (1992).

- [41] Crystal structure was rendered using VESTA code. K. Momma and F. Izumi, “VESTA3 for three-dimensional visualization of crystal, volumetric and morphology data,” *J. Appl. Crystallogr.* **44**, 1272 (2011).
- [42] M. Aono, T. Tanaka, E. Bannai, C. Oshima, and S. Kawai, “Surface states of LaB<sub>6</sub>(001) as revealed by angular-resolved ultraviolet photoelectron spectroscopy,” *Phys. Rev. B* **16**, 3489 (1977).
- [43] Z.-H. Zhu, A. Nicolaou, G. Levy, N. P. Butch, P. Syers, X. F. Wang, J. Paglione, G. A. Sawatzky, I. S. Elfimov, and A. Damascelli, “Polarity-driven surface metallicity in SmB<sub>6</sub>,” *Phys. Rev. Lett.* **111**, 216402 (2013).
- [44] C. Herring and M. H. Nichols, “Thermionic emission,” *Rev. Mod. Phys.* **21**, 185 (1949).
- [45] A. Modinos, “Theory of thermionic emission,” *Surf. Sci.* **115**, 469 (1982).